

A method for measuring heteronuclear (1H-13C) distances in high speed MAS NMR

Rossum, B.J. van; Groot, H.J.M. de; Ladizhansky, V.; Vega, S.; Groot, C.P. de

Citation

Rossum, B. J. van, Groot, H. J. M. de, Ladizhansky, V., Vega, S., & Groot, C. P. de. (2000). A method for measuring heteronuclear (1H-13C) distances in high speed MAS NMR. *Journal Of The American Chemical Society*, 122(14), 3465-3472. doi:10.1021/ja992714j

Version: Publisher's Version

License: Licensed under Article 25fa Copyright Act/Law (Amendment Taverne)

Downloaded from: https://hdl.handle.net/1887/3464759

Note: To cite this publication please use the final published version (if applicable).

A Method for Measuring Heteronuclear (¹H-¹³C) Distances in High Speed MAS NMR

B.-J. van Rossum,† C. P. de Groot,† V. Ladizhansky,‡ S. Vega,‡ and H. J. M. de Groot*,†

Contribution from the Leiden Institute of Chemistry, Gorlaeus Laboratories, Leiden University, PO Box 9502, 2300 RA Leiden, The Netherlands, and the Chemical Physics Department, Weizmann Institute of Science, 76100 Rehovot, Israel.

Received July 30, 1999. Revised Manuscript Received January 21, 2000

Abstract: Magic angle spinning (MAS) NMR structure determination is rapidly developing. We demonstrate a method to determine ¹H-¹³C distances r_{CH} with high precision from Lee-Goldburg cross-polarization (LG-CP) with fast MAS and continuous LG decoupling on uniformly ¹³C-enriched tyrosine · HCl. The sequence is γ -encoded, and ${}^{1}H^{-13}C$ spin-pair interactions are predominantly responsible for the polarization transfer while proton spin diffusion is prevented. When the CP amplitudes are set to a sideband of the Hartmann-Hahn match condition, the LG-CP signal builds up in an oscillatory manner, reflecting coherent heteronuclear transfer. Its Fourier transform yields an effective ¹³C frequency response that is very sensitive to the surrounding protons. This ¹³C spectrum can be reproduced in detail with MAS Floquet simulations of the spin cluster, based on the positions of the nuclei from the neutron diffraction structure. It is symmetric around $\omega = 0$ and yields two well-resolved maxima. Measurement of CH distances is straightforward, since the separation $\Delta\omega$ $/2\pi$ between the maxima for a single $^{1}H^{-13}C$ pair is related to the internuclear distance according to r_{CH} $a(\Delta\omega/2\pi)^{-1/3}$, with $a=25.86\pm0.01$ Å Hz^{1/3}. For the ¹H directly bonded to a ¹³C, the magnetization is transferred in a short time of $\sim 100 \,\mu s$. After this initial rapid transfer period, the COOH, OH, or NH₃ that are not directly bonded to a ¹³C transfer magnetization over long distances. This offers an attractive route for collecting long-range distance constraints and for the characterization of intermolecular hydrogen bonding.

Introduction

Magic angle spinning nuclear magnetic resonance (MAS NMR) techniques for structure determination of uniformly enriched compounds or multispin clusters in solid-type biological systems without translation symmetry are rapidly developing. The measurement of heteronuclear (1H-13C) intermolecular distances is potentially an important tool in structure determination of solids, since it can provide restraints that can be used for structure refinement by modeling. Information about the internuclear distance between two spins can be deduced from the strength of the heteronuclear (${}^{1}H^{-13}C$) dipolar interaction. For a static sample, the dipolar interaction between the two spins of a heteronuclear spin-pair yields a symmetric Pake doublet,² in which the separation between the two maxima provides a direct measure for the heteronuclear dipolar coupling strength. MAS, however, averages the heteronuclear dipolar interactions and gives rise to a pattern of spinning sidebands, with the relative intensities of the spinning sidebands determined by both the dipolar interaction and the chemical shift.³ For small shift anisotropies, the envelope of the sideband intensities reflects the static Pake pattern at low spinning speeds $\omega_r/2\pi < 3$ kHz, while at high MAS rates $\omega_r/2\pi > 10$ kHz the dipolar interaction is substantially reduced by the sample spinning, like the chemical shift anisotropy (CSA).

One way to determine heteronuclear dipolar couplings with MAS is to perform separated local field spectroscopy. In this technique the dipolar interaction is separated from the chemical shift interaction, resulting in 2-dimensional (2-D) spectra with the chemical shift of each nucleus in one dimension correlated with its dipolar coupling to neighboring spins in the second dimension. 3-11 However, this high-resolution method requires slow MAS to ensure sufficient sideband intensity to obtain the strength of the dipolar interactions.^{3,5} On the other hand, to achieve a good resolution in the chemical shift dimension for multispin clusters at high magnetic field strengths, fast MAS is required to suppress the CSA.

In this paper we present a method that can be applied to extract heteronuclear distances in uniformly 13C-enriched ([U-¹³C]) compounds with good precision from cross-polarization (CP) build-up curves, recorded at high MAS rates 10 kHz $<\omega_{\rm r}/2\pi$ < 15 kHz under simultaneous suppression of the ¹H homonuclear dipolar interactions. The Fourier transform of the

[†] Leiden University.

[‡] Weizmann Institute.

⁽¹⁾ van Rossum, B.-J.; Boender, G. J.; Mulder, F. M.; Raap, J.; Balaban, T. S.; Holzwarth, A.; Schaffner, K.; Prytulla, S.; Oschkinat, H.; de Groot, H. J. M. Spectrochim. Acta A 1998, 54, 1167

⁽²⁾ Pake, G. E. J. Chem. Phys. 1948, 16, 327.

⁽³⁾ Roberts, J. E.; Harbison, G. S.; Munowitz, M. G.; Herzfeld, J.; Griffin, R. G. J. Am. Chem. Soc. 1987, 109, 4163.

⁽⁴⁾ Munowitz, M. G.; Griffin, R. G.; Bodenhausen, G.; Huang, T. H. J. Am. Chem. Soc. 1981, 103, 2529.

⁽⁵⁾ Munowitz, M. G.; Griffin, R. G. J. Chem. Phys. 1982, 76, 2848.

⁽⁶⁾ Munowitz, M.; Aue, W. P.; Griffin, R. G. J. Chem. Phys. 1982, 77, 1686.

⁽⁷⁾ Munowitz, M. G.; Griffin, R. G. J. Chem. Phys. 1983, 78, 613.

⁽⁸⁾ Kolbert, A. C.; de Groot, H. J. M.; Levitt, M. H.; Munowitz, M. G.; Roberts, J. E.; Harbison, G. S.; Herzfeld, J.; Griffin, R. G. Multinuclear Magnetic Resonance in Liquids and Solids-Chemical Applications; Kluwer Academic Publishers: The Netherlands, 1990; p 339.

⁽⁹⁾ Kolbert, A. C.; de Groot, H. J. M.; Griffin, R. G. J. Magn. Reson. **1989**, 85, 60.

⁽¹⁰⁾ Wu, C. H.; Ramamoorthy, A.; Opella, S. J. J. Magn. Reson. A 1994,

⁽¹¹⁾ Ramamoorthy, A.; Opella, S. J. Solid State Nucl. Magn Reson. 1995,

time-oscillatory magnetization build-up curves provides dipolar broadened response profiles reflecting the heteronuclear (¹H–¹³C) dipolar coupling strengths that can be related to internuclear distances between the coupled spin-pairs.

Theoretical Background

In this work the time-evolution of the signal intensity of a $^{13}\mathrm{C}$ spin S during CP/MAS with Lee–Goldburg (LG) irradiation applied to a number of I spins ($^1\mathrm{H}$) is analyzed. The LG irradiation significantly suppresses the $^1\mathrm{H}$ homonuclear dipolar interactions and relies on the application of an off-resonance RF field to the $^1\mathrm{H}$ spins, in such a way that the effective field in the rotating frame is inclined at the magic angle $\theta_{\rm m}=54.7^{\circ}$ with respect to the static magnetic field H_0 along the z-axis. 12 We restrict the theoretical description to a two-spin system that consists of a spin S coupled to a single spin I and rotating with $\omega_{\rm r}/2\pi$. The description of spin systems containing more than one I spin is treated numerically. 13

The spin Hamiltonian in the doubly rotating frame for the two-spin system during the mixing time of the Lee—Goldburg CP (LG-CP)^{10,12,14,15} experiment can be represented as

$$H = \omega_{1I}I_r + \omega_{1S}S_r + \Delta\omega_{I}I_r + b(t)I_rS_r \tag{1}$$

where $\omega_{\rm II} = -\gamma_{\rm I} H_{\rm II}$ and $\omega_{\rm IS} = -\gamma_{\rm S} H_{\rm IS}$ are the RF fields on the *I* and *S* spins, respectively, and where $\Delta \omega_{\rm I} = \omega_{\rm RF} - |\omega_{\rm 0I}|$, with $\omega_{\rm 0I} = -\gamma_{\rm I} H_{\rm 0I}$, is the frequency offset of the RF irradiation of the *I* spin. For LG irradiation, the condition $\tan^{-1}[|\omega_{\rm II}|/\Delta\omega_{\rm I}] = \theta_{\rm m}$ holds. The last term in eq 1 represents the heteronuclear dipolar interaction $H_{\rm IS}$ between the two spins, with 16

$$b(t) = 2\omega_{\rm d}[G_1\cos(\omega_{\rm r}t + \phi) + G_2\cos(2\omega_{\rm r}t + 2\phi)]$$

$$\omega_{\rm d} = -\frac{\mu_0}{4\pi} \frac{\gamma_1 \gamma_S \hbar^2}{r_{\rm IS}^3} \tag{2}$$

In the tilted frame, defined by the transformation $\exp\{-i\theta_{\rm m}I_y\}$ $\exp\{-i(\pi/2)S_y\}$, the tilted spin Hamiltonian can be written as $H_{\rm T}=H_0+H_1(t)$, where

$$H_0 = \omega_{\text{eff,I}} I_z + \omega_{1S} S_z$$

$$H_1(t) = b(t) (\sin(\theta_m) I_x S_x - \cos(\theta_m) I_z S_x)$$
(3)

with the effective field $\omega_{\rm eff,I} = -(\omega_{11}^2 + \Delta\omega_{1}^2)^{1/2}$. The time independent part H_0 can be removed from the Hamiltonian by transformation to the interaction frame, according to $H_1^* = \exp\{iH_0t\}H_1 \exp\{-iH_0t\}$. The resulting expression can be simplified if the $n=\pm 1$ Hartmann–Hahn (HH) matching condition is fulfilled, that is, when $\omega_{\rm eff,I} - \omega_{1S} = \pm \omega_{\rm r}$, and if oscillating terms of the form $\cos \omega_{\rm r}t$, $\cos 2\omega_{\rm r}t$ etc., are neglected compared to the time-independent term. For the condition $\omega_{\rm eff,I} - \omega_{1S} = +\omega_{\rm r}$ this leads to the following expression for the Hamiltonian representing the heteronuclear dipolar interaction

$$H_{\rm l}^* = \frac{\delta}{4} \left[I_+ S_- \exp(i\phi) + I_- S_+ \exp(-i\phi) \right]$$
 (4)

with $\delta \equiv G_1 \omega_d \sin(\theta_m)$. The factor $\sin(\theta_m)$ in H_1^* scales the heteronuclear dipolar interaction.

Following excitation of the *I* spins, the density operator at the beginning of the LG-CP period in the interaction frame can be written as $\rho_0 = -Z^{-1}\beta_L\omega_{0l}I_z$, with $\beta_L = 1/k_BT$. The time-evolution of ρ under H_1^* can be calculated using $\rho(t) = \exp(-iH_1^*t)\rho_0 \exp(iH_1^*t)$, which leads to the following expression, in matrix-notation in the product basis $|m_l m_S\rangle$

$$\rho(t) = -\frac{1}{4} Z^{-1} \beta_{L} \omega_{01}.$$

$$\begin{pmatrix} 1/2 & 0 & 0 & 0 \\ 0 & -1/2 & 0 & 0 \\ 0 & 0 & 1/2 \cos^{1}/2 \delta t & -1/2 \exp(i\phi) \sin^{1}/2 \delta t \\ 0 & 0 & -1/2 \exp(-i\phi) \sin^{1}/2 \delta t & -1/2 \cos^{1}/2 \delta t \end{pmatrix} \begin{vmatrix} 1++\rangle \\ |+-\rangle \\ |-+\rangle (5)$$

The S-spin signal S(t) can be evaluated by calculation of the expectation value of S_z , according to $\langle S_z(t) \rangle = Tr(\rho(t)S_z)$, which leads to

$$S(t) = -\frac{1}{4} Z^{-1} \beta_{L} \omega_{0I} \left(1 - \cos \frac{1}{2} \delta t \right) = -\frac{1}{4} Z^{-1} \beta_{L} \omega_{0I} \left(1 - \frac{1}{2} \exp \left(+ \frac{i}{2} \delta t \right) - \frac{1}{2} \exp \left(- \frac{i}{2} \delta t \right) \right)$$
(6)

An identical expression is found for the $\omega_{\rm eff,I}-\omega_{\rm 1S}=-\omega_{\rm r}$ HH condition. Hence, during the LG-CP, the *S*-spin signal oscillates with angular frequency $^{1}/_{2}\delta$ around the average value $^{-1}/_{4}Z^{-1}\beta_{\rm L}\omega_{\rm 0I}$, and Fourier transformation of $S(t)+^{1}/_{4}Z^{-1}\beta_{\rm L}\omega_{\rm 0I}$ results in a spectrum with two singularities at frequencies $\omega=\pm^{1}/_{2}\delta=\pm\,{\rm G}_{\rm 1}\omega_{\rm d}$ sin $\theta_{\rm m}$.

The expectation value for $\langle S_z(t) \rangle$ has been evaluated for a single crystallite. For a powder sample, it should be integrated over all crystallites. With $G_1 = {}^{3}/_{4} \sin(2\theta_{\rm m}) \sin(2\theta_{ij}), {}^{16}$ and θ_{ij} the angle between the internuclear vector connecting spins i and j and the rotor axis, we can write $\omega(\theta_{ij}) = {}^{1}/_{2}\delta_{0} \sin(2\theta_{ij}),$ with $\delta_0 \equiv {}^{3}/_{4}\omega_{\rm d} \sin(\theta_{\rm m}) \sin(2\theta_{\rm m}) = \omega_{\rm d} \cos(\theta_{\rm m})$. The powder average can be evaluated using $S(\omega) = P(\theta_{ij})/|{\rm d}\theta_{ij}(\omega)/{\rm d}\omega|$, with $P(\theta_{ij})$ the angular distribution function. To Since the interaction is axially symmetric, we simply have $P(\theta_{ij}) = \sin \theta_{ij}$, which leads to

$$S(\omega) = \frac{\sqrt{\frac{1}{2} - \sqrt{\frac{1}{4} - (\omega/\delta_0)^2} + \sqrt{\frac{1}{2} + \sqrt{\frac{1}{4} - (\omega/\delta_0)^2}}}{2\sqrt{\frac{1}{4} - (\omega/\delta_0)^2}}$$
(7)

with $-\delta_0/2 \le \omega \le \delta_0/2$.

The $S(\omega)$ is plotted in Figure 1. It represents the LG-CP S-spin spectrum for the IS spin-pair, which is obtained after Fourier transformation of the time-oscillating S-spin signal build-up. The shape resembles a static Pake-pattern, although the characteristic high-frequency "ears" are missing. The frequency splitting between the two maxima equals δ_0 , which is related to the heteronuclear distance $r_{\rm IS}$ via $\omega_{\rm d}$ in eq 2.

⁽¹²⁾ Lee, M.; Goldburg, W. I. Phys. Rev. A 1965, 140, 1261.

⁽¹³⁾ Ray, S.; Ladizhansky, V.; Vega, S. *J. Magn. Reson.* **1998**, *135*, 427. (14) Caravatti, P.; Bodenhausen, G.; Ernst, R. R. *Chem. Phys. Lett.* **1982**,

⁽¹⁴⁾ Caravatti, P.; Bodenhausen, G.; Ernst, R. R. Chem. Phys. Lett. **1982** 89, 363.

⁽¹⁵⁾ van Rossum, B.-J.; Prytulla, S.; Oschkinat, H.; de Groot, H. J. M. *Magnetic Resonance and Related Phenomena*; Technische Universität: Berlin, 1998; Vol. 1, p 38.

⁽¹⁶⁾ Bennet, A. E.; Griffin, R. G.; Vega, S. NMR-Basic Principles and Progress; Springer-Verlag: Berlin, 1994; Vol. 33, p 1.

⁽¹⁷⁾ Schmidt-Rohr, K.; Spiess, H. Multidimensional Solid-state NMR and Polymers; Academic Press: London, 1994.

⁽¹⁸⁾ Bertani, P.; Raya, J.; Reinheimer, P.; Goneon, R.; Delmotte, L.; Hirschinger, J. Solid State Nucl. Magn. Reson. 1999, 13, 219.

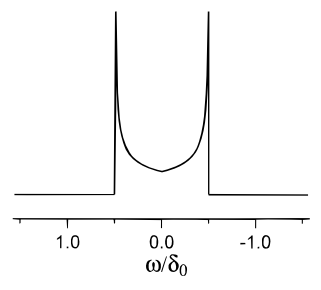


Figure 1. Powder pattern of the LG-CP *S*-spin spectrum according to eq 7, representing the Fourier transform of the time oscillatory signal build-up during LG-CP.

The eq 7 is the same as rotational resonance recoupling sequence. ¹⁹ Here we start with a dipolar Hamiltonian (1) in the doubly rotating frame with a time-dependent dipolar interaction b(t) given by eq 2. The matching of the b(t) gives rise to modes that oscillate with frequencies $n\omega_r$. The I_z and S_z rotate in the interaction frame and when the LG-CP is set to a first sideband of the HH match condition $\omega_{\text{eff,I}} - \omega_{1\text{S}} = \pm \omega_r$, the difference in rotation frequency matches the ω_r mode of the b(t). This is similar to the rotational resonance recoupling. There the oscillating modes of a dipolar Hamiltonian b(t) in the normal rotating frame are matched to the rotation frequency $n\omega_r$ of the S_z in the RF interaction frame. This leads to a similar effective Hamiltonian and the same powder spectrum $S(\omega)$. ¹⁹

Material and Methods

The solid-state CP/MAS spectra were recorded with a DMX-600 and a DMX-750 spectrometer, equipped with 4 mm double resonance CP/MAS probes (Bruker, Karlsruhe, Germany). For the experiments with the DMX-600 instrument, a home-built spinning speed controller was used to stabilize the spinning speed.²⁰ The pulse sequences for the 2-D and 3-dimensional (3-D) heteronuclear polarization transfer experiments are shown in Figure 2 A and B, respectively. The 2-D sequence starts with a magic angle preparation pulse that puts the ¹H polarization at the magic angle with respect to the z-axis and parallel to the direction of the effective field in the rotating frame during the LG-CP. 10,12,14,15 Alternatively, a 90° proton preparation pulse can be applied, which improves elimination of probe ring-down via phase cycling, at the expense of a ~20% reduction of the signal. The 2-D dataset presented in this paper was recorded with a magic angle preparation pulse, while the 3-D experiment discussed below effectively makes use of the variant with a 90° preparation pulse. Following ¹H excitation in the 2-D experiment, LG-CP is applied to transfer the magnetization from the protons to the carbons during a variable time t_1 . The LG-CP spin-locks the ¹H signal along the effective field, while the ¹³C spins can be locked on-resonance in the xy-plane. In this way, heteronuclear spin-locking is achieved, while simultaneously the ¹H homonuclear dipolar interactions are significantly suppressed. Fourier transformation with respect to t_1 provides the ¹³C heteronuclear dipolar interaction dimension of the correlation experiment. A moderate proton RF power corresponding with an ¹H nutation frequency of 60 kHz was used for the LG-CP. The 13 C free induction decays (FIDs) were recorded in the t_2 domain, using proton decoupling with the two-pulse phase modulation (TPPM) scheme.²¹ The HH matching profile during MAS was mapped by sweeping the ¹³C RF power while following the ¹³C signal intensity in t_2 . In this way, the $n = \pm 1$ HH matching conditions for the LG-CP can be determined experimentally.

The pulse program for the 3-D experiment in Figure 2B combines frequency-switched Lee-Goldburg (FSLG) decoupled ¹H-¹³C hetero-

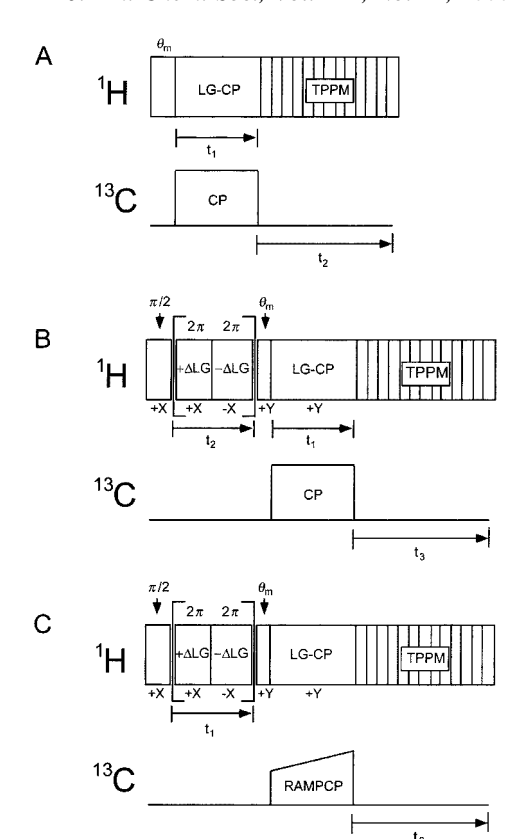


Figure 2. Pulse programs used to study heteronuclear (${}^{1}H^{-13}C$) polarization exchange in two (A) and three dimensions (B), and for 2-D FSLG decoupled ${}^{1}H^{-13}C$ heteronuclear dipolar correlation spectroscopy with LG-CP (C).

nuclear dipolar correlation spectroscopy in t2 and t3 with the 1H excitation and LG-CP evolution in t_1 of the pulse program shown in Figure 2A. After ¹H excitation, the protons are allowed to evolve for a time t2 with FSLG irradiation to suppress the 1H homonuclear dipolar couplings., 1,22,23 The plane of precession is perpendicular to an axis that is inclined at the magic angle with respect to the z-axis, and the magic angle y-pulse at the end of t2 rotates components of the ¹H signal into the xy-plane. The phases of the proton preparation pulse, the FSLG sequence and the magic angle pulse are varied according to a time proportional phase incrementation scheme to simulate phase sensitive detection in t2.24 The LG-CP selects and spin-locks the component of the ¹H signal that is parallel to the effective field. Following the heteronuclear polarization transfer during t_1 , the ¹³C FIDs are recorded in t_3 with TPPM decoupling. The resulting 3-D ${}^{1}H-{}^{1}H-{}^{13}C$ dataset can be represented as a series of heteronuclear correlation spectra recorded with different LG-CP contact times in t_1 . The contributions of the various protons in the vicinity of a ¹³C to the magnetization exchange can be studied separately in the ¹H frequency domain after Fourier transformation in t_1 .

Figure 2C shows the pulse program for 2-D $^{1}H-^{13}C$ heteronuclear dipolar correlation spectroscopy. The protons evolve during t_1 under suppression of the ^{1}H homonuclear dipolar interactions with the FSLG. LG-CP was used to establish selective heteronuclear polarization transfer during a long CP mixing time of 1.5 ms, 15 while a ramped CP spin-lock pulse on the carbon nuclei was applied to broaden the CP matching profile at high MAS rates. 25

In a convenient way to determine the scaling factor for a 2-D $^1H-^{13}C$ heteronuclear dipolar correlation spectrum, the slope was determined

⁽¹⁹⁾ Levitt, M. H.; Oas, T. G., Griffin, R. G. Isr. J. Chem. 1988, 28, 271

⁽²⁰⁾ De Groot, H. J. M.; Copié, V.; Smith, S. O.; Allen, P. J.; Winkel, C.; Lugtenburg, J.; Herzfeld, J.; Griffin, R. G. *J. Magn. Reson.* **1988**, 77, 251.

⁽²¹⁾ A. E.; Rienstra, C. M.; Auger, M.; Lakshmi, K. V.; Griffin, R. G. J. Chem. Phys. **1995**, 103, 6951.

⁽²²⁾ Bielecki, A.; Kolbert, A. C.; Levitt, M. H. Chem. Phys. Lett. 1989, 155, 341.

⁽²³⁾ van Rossum, B.-J.; Förster, H.; de Groot, H. J. M. J. Magn. Reson. **1997**, 124, 516.

⁽²⁴⁾ Marion, D.; Wüthrich, K. *Biochem. Biophys. Res. Com.* **1983**, *113*, 967.

⁽²⁵⁾ Metz, G.; Wu, X.; Smith, S. O. J. Magn. Reson. A 1994, 110, 219.

Figure 3. The chemical structure of tyrosine HCl with IUPAC numbering scheme.

of a plot of scaled L-tyrosine+HCl proton chemical shifts obtained from a FSLG experiment against the corresponding nonscaled proton chemical shifts obtained from a correlation spectrum recorded with the CP/WISE technique in a high magnetic field and with fast MAS.^{26,27}

Simulations of LG-CP MAS ¹³C signals are performed using an IBM SP2 computer following the method described by Ray et al. ¹³ Coordinates for carbon and hydrogen atoms in L-tyrosine·HCl (Figure 3) were taken from the high-resolution neutron diffraction structure. ²⁸

Results

The aim of this paper is to demonstrate that the timeoscillatory build-up of the carbon signal during CP for fast MAS directly provides the heteronuclear (¹H-¹³C) dipolar coupling strength, which can be related to a distance r_{CH} . To this end, interactions other than the heteronuclear dipolar coupling should be removed from the spin Hamiltonian. The locking of the ¹H and ¹³C spins during CP suppresses the chemical shift evolution of both spin types, while the ¹³C homonuclear dipolar couplings average to zero at high MAS rates. Therefore, the two major remaining interactions that determine the time-evolution of the spin system are the ¹H homonuclear and the ¹H-¹³C heteronuclear dipolar couplings, ignoring the weaker J couplings. The ¹H homonuclear dipolar interactions can be removed successfully from the spin Hamiltonian by application of the LG-CP. This will prevent ¹H homonuclear spin diffusion during CP, while ¹H-¹³C polarization exchange can proceed mediated by the heteronuclear dipolar interactions.

Figure 4 shows a 2-D experiment recorded with the pulse sequence in Figure 2A from [U-¹³C] L-tyrosine•HCl with an ¹H frequency of 600 MHz using $\omega_r/2\pi = 12$ kHz. The LG-CP was adjusted for the n = -1 HH matching condition. An experiment using the n = +1 matching condition yielded virtually identical results (data not shown). The n = 0 condition should not be chosen, since this results in a reduction of the effective heteronuclear dipolar interactions, which will lead to a much less efficient polarization transfer.²⁹

The data in Figure 4 were processed with a Fourier transform in the ¹³C dimension only. In this series of ¹³C spectra the isotropic carbon chemical shifts are correlated with the variation of the signal intensity during the LG-CP mixing time. In this way the LG-CP build-up curves are separated according to their carbon shifts. Figure 5 shows the F1 slices correlated with the 2-¹³C response at 56.3 ppm (Figure 5A) and with the 3-¹³C signal at 36.6 ppm (Figure 5B). The CP signal builds up in time in an oscillatory manner.³⁰ Since the ¹H homonuclear dipolar interactions and the chemical shift evolution of both spin types are suppressed during the LG-CP, the oscillations reflect evolution of the ¹³C magnetization and coherent transfer of ¹H polarization.^{10,14}

The Fourier transforms of the LG-CP build-up curves of the 2-13C (Figure 5C) and the 3-13C (Figure 5D) carbons yield effective carbon responses in the frequency domain. Prior to Fourier transformation, the data were corrected for the vertical baseline offset. The LG-CP carbon spectrum for the CH moiety in Figure 5C is very similar to the theoretically predicted response in Figure 1 for an isolated CH spin-pair, and is modulated with spectral intensities at integral multiples of the rotor speed $\omega_r/2\pi = 12$ kHz. It appears that the major contribution to this spectrum originates from dipolar transfer within the CH spin-pair, while the lower frequency intensities can be attributed to transfer from weakly coupled remote protons. From the peak-to-peak distance $\Delta\omega/2\pi$ between the maxima, a LG-CP dipolar coupling frequency $\Delta\omega/2\pi = 12~070$ Hz is estimated for the CH pair. The LG-CP carbon spectrum for the CH₂ group is more complicated and exhibits a doublet structure that gives rise to a total of four maxima (Figure 5D). The splitting for the interior pair of maxima equals to a frequency $\Delta\omega/2\pi = 12\,040$ Hz.

In the virtual environment of the computer, an ideal LG decoupling is easily mimicked by omitting the ¹H homonuclear dipolar interactions in the simulations. In addition, the ${}^{1}H-{}^{13}C$ heteronuclear dipolar interaction is scaled in the simulations by a factor $\sin(\theta_{\rm m}) = 0.817$. To follow the experiment, the simulations were performed for the n = -1 HH matching condition. The simulations for the CH moiety were done for a two-spin cluster that consisted of a ¹³C spin coupled to a directly bonded proton and for a six-spin cluster of a ¹³C spin coupled to a total of five protons, taking into account the coordinates of the five nearest protons according to the neutron diffraction structure.²⁸ Likewise, for the CH₂ group the simulations were performed for a ¹³C spin with its two covalently bonded protons, and for a spin cluster containing three additional remote protons. Powder spectra were constructed by adding the spectral intensities of a total of 1154 different crystal orientations.

Simulations of the LG-CP carbon spectra for the 2-CH and 3-CH₂ moieties are shown in Figure 5 E and F, respectively. The LG-CP carbon spectra for the spin systems comprising five protons are indicated with dotted lines. Since all relaxation processes were ignored in the simulations, the simulated spectra have been artificially broadened in order to allow for a straight comparison with the experimental data. From the envelope of the experimental magnetization build-up curve of the 2- 13 C in Figure 5A, a pseudo transverse relaxation time $T_2{}^{'}\approx 0.4$ ms was estimated. From this, a Lorentzian line width $\Gamma\approx 800$ Hz was derived according to $\Gamma=(\pi T_2{}^{'})^{-1}$, which was used in an Lorentzian apodization of the simulated build-up curves in the time domain.

The overall similarity between experimental and simulated responses is encouraging and many essential features of the LG-CP carbon spectra in Figure 5 C and D can be recognized in the MAS Floquet simulations of the heteronuclear spin clusters spinning with 12 kHz (Figure 5 E and F). For the CH moiety, the characteristic powder pattern envelope in Figure 1 transpires (Figure 5E). Additional intensity is present in the form of narrow lines at integral multiples of the MAS rate. The simulations confirm that the main broad contribution to the spectrum arises from the dipolar interactions with the directly bonded proton, while a weaker and narrower response in the center around 0 Hz is associated with dipolar transfer from the remote protons. It was observed during the course of the simulations that the dipolar couplings to remote protons do have a minor effect on the shape of the response from the strongly coupled CH spinpair. Adding an increasing number of distant protons in the

⁽²⁶⁾ Schmidt-Rohr, K.; Clauss J.; Spiess, H. W. Macromolecules 1992, 25, 3273.

⁽²⁷⁾ van Rossum, B.-J.; Boender, G. J.; de Groot, H. J. M. J. Magn. Reson. A 1996, 120, 274.

⁽²⁸⁾ Frey, M. N.; Koetzle, T. F.; Lehmann, M. S.; Hamilton, W. C. J. Chem. Phys. **1973**, 58, 2547.

⁽²⁹⁾ Marks, D.; Vega, S. J. Magn. Reson. A 1996, 118, 157.

⁽³⁰⁾ Müller, L.; Kumar, A.; Baumann, T.; Ernst, R. R. Phys. Rev. 1974, 32, 1402.

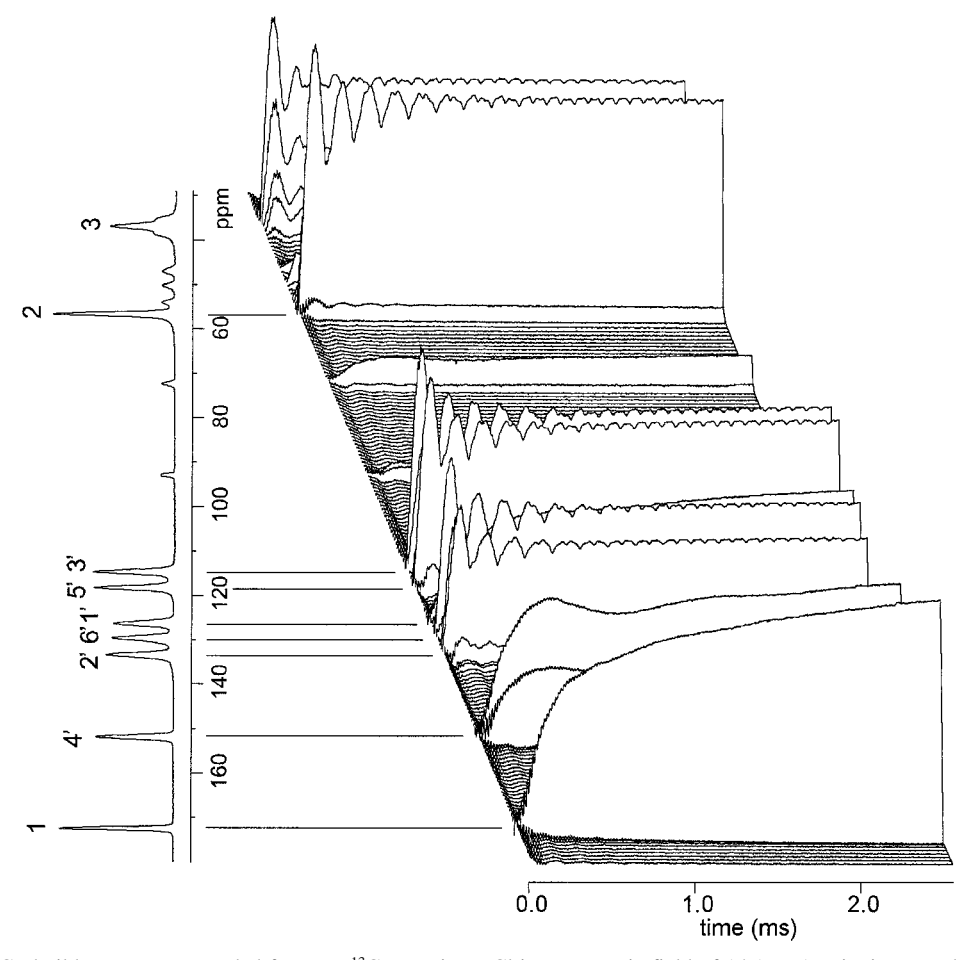


Figure 4. 2-D LG-CP build-up curves recorded from [U- 13 C] tyrosine HCl in a magnetic field of 14.1 T. A spinning speed $\omega_r/2\pi = 12$ kHz was applied. The LG-CP was adjusted for the n = -1 HH matching condition.

simulation leads to a gradual broadening of the LG-CP response and to a shift of the maxima to higher frequencies. The LG-CP dipolar frequencies $\Delta\omega/2\pi$ for the spin-clusters with one and five protons in Figure 5E are 12 780 Hz and 12 920 Hz, respectively. These values compare well with the splitting $\delta_0=\omega_{\rm d}\cos(\theta_{\rm m})$ predicted from the theory. This value equals to $\delta_0=13\ 100$ Hz, for the same distance $r_{\rm CH}=1.1$ Å that was used in the simulations.

The major contribution to the doublet structure in the simulation of the LG-CP response for the CH₂ group in Figure 5F can be attributed to polarization exchange within the CH₂ moiety. Just as for the CH, the remote protons contribute mainly to the central part of the spectrum, and they have a small broadening effect on the CH₂ shape. For a simulation of an isolated CH₂ pair, the LG-CP dipolar frequency $\Delta\omega/2\pi =$ 13 240 Hz is defined as the separation between the maxima. For a simulation of a spin system containing five protons this increases to $\Delta\omega/2\pi = 13\,310$ Hz. In the simulations the interior doublet is more intense than the exterior part. This is in good qualitative agreement with the experimental data. Other features are also qualitatively reproduced, for example, the intensity around ± 16 kHz, which was not observed for the CH moiety, and high-frequency shoulders at ± 7300 Hz. The agreement between the experimental and simulated splittings $\Delta\omega/2\pi$ in Figure 5 will be discussed in the next section.

Figure 6 shows the polarization build-up for the 4'- 13 C and its Fourier transform. The 4'- 13 C is a quaternary carbon and therefore only weakly dipolar coupled to protons (Figure 6A). In the Fourier transform of the slow oscillations in the time domain signal in Figure 6B, three frequency components appear,

which can be assessed most accurately by taking the second derivative of the data. This is illustrated in Figure 6C, from which the splittings $\Delta\omega/2\pi=2100\pm25$ Hz and $\Delta\omega/2\pi=1150\pm100$ Hz are obtained. A relatively large uncertainty in $\Delta\omega/2\pi$ of $\sim\!100$ Hz is estimated for the lower frequency component, since the value depends on the baseline correction during the data processing.

According to the neutron diffraction data, there are four protons in the vicinity of the 4'-C.²⁸ The shortest intramolecular distances are to the 4'-OH phenolic proton (1.982 Å), and the two aromatic protons 3'-H (2.150 Å) and 5'-H (2.148 Å). In addition, the oxygen of the 4' hydroxyl group forms an intermolecular hydrogen bond to the 1-OOH of a neighboring molecule in the crystal, with the hydrogen bonding proton located at a distance of 2.521 Å from the 4'-C (Figure 7).

Interestingly, we have observed that the 4'- 13 C predominantly receives its LG-CP polarization through intramolecular transfer from the 4'- 0^1 H proton and intermolecular transfer from the 1-OO 1 H proton, while the 3'- 1 H and 5'- 1 H predominantly exchange polarization with 3'- 13 C and 5'- 13 C and appear to contribute little to the initial 4'- 13 C signal build-up. Figure 8 shows a contour plot of a heteronuclear dipolar correlation spectrum recorded with the pulse scheme in Figure 2C from [U- 13 C] L-tyrosine•HCl. The spectrum was obtained with FSLG 1 H homonuclear dipolar decoupling during the proton evolution, 22,23 at a MAS rate $\omega_r/2\pi=15$ kHz and using a high magnetic field strength of 17.6 T corresponding with an 1 H NMR frequency of 750 MHz. Selective magnetization transfer was achieved by applying a LG-CP contact time of 1.5 ms. 14 By using the procedure described in the Materials and Methods,

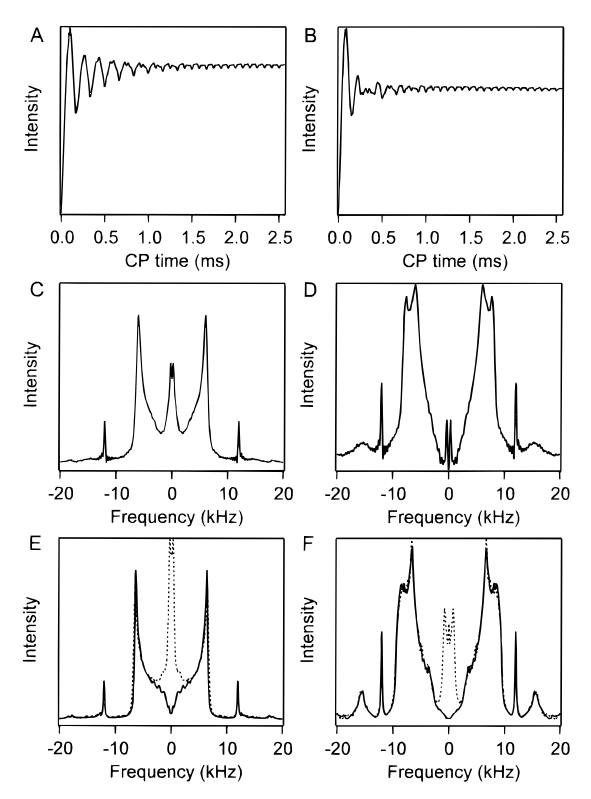


Figure 5. LG-CP build-up curves and the Fourier transforms for the 2-CH (A,C) and 3-CH₂ (B,D) moiety, extracted from the 2-D experiment in Figure 4. MAS Floquet simulations of the LG-CP carbon spectra for spin systems consisting of a ¹³C spin with its covalently bonded protons only (solid lines) or a ¹³C spin with its five nearest protons (dotted lines) are shown for 2-CH (E) and 3-CH₂ (F), apodized with a 800 Hz exponential broadening.

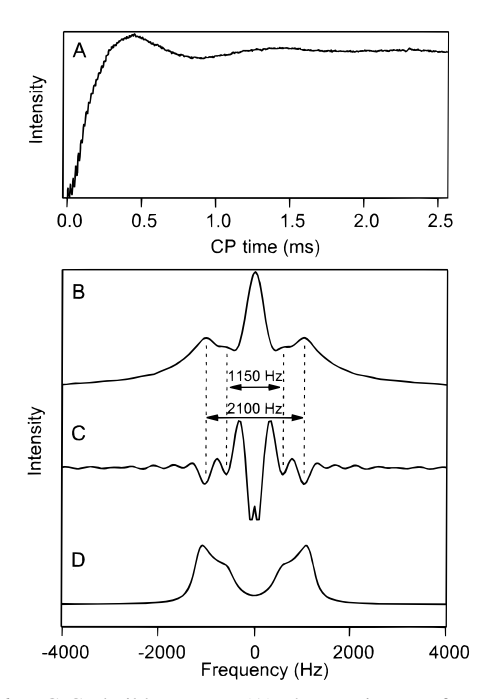


Figure 6. LG-CP build-up curve (A), the Fourier transform (B), and the second derivative of the Fourier transform (C) for the 4′-¹³C, extracted from the 2-D experiment in Figure 4. MAS Floquet simulation of the LG-CP carbon spectrum for a spin system consisting of the 4′-¹³C, the 4′-O¹H and the 1-OO¹H (D).

a scaling factor of 0.50 was found for the FSLG decoupled heteronuclear correlation experiment. This is somewhat lower than the theoretical factor $\cos(\theta_{\rm m})=1/\sqrt{3}=0.577,^{12}$ and

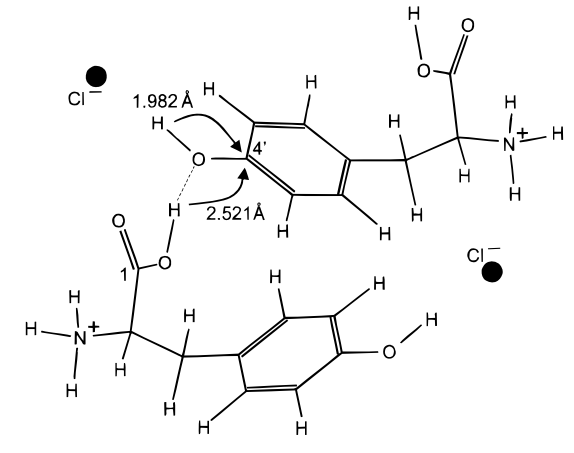


Figure 7. Arrangement of crystalline L-tyrosine HCl according to the neutron diffraction structure.²⁸ The dashed line indicates the intermolecular hydrogen bonding network of 1-OOH to 4'-OH.

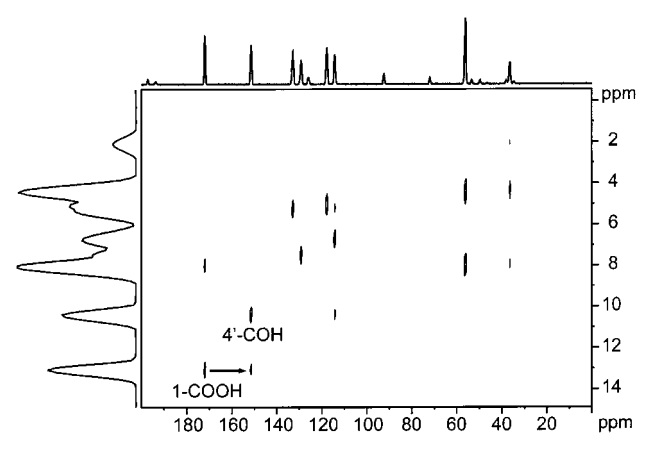


Figure 8. Contour plot of a 2-D FSLG decoupled heteronuclear (${}^{1}H-{}^{13}C$) dipolar correlation spectrum from [U- ${}^{13}C$]-L-tyrosine•HCl. The data were recorded in a magnetic field of 17.6 T using a spinning speed $\omega_r/2\pi=15$ kHz. A LG-CP time of 1.5 ms was applied.

improvement of the resolution may be reached by fine-tuning of the LG offset frequencies. However, we felt no need for additional parameter optimization, for the reason that the lines are already fully resolved in the proton dimension in this dataset.

As can be observed from the 2-D spectrum, the 4'-13C response has a strong heteronuclear correlation with the 4'-0¹H proton and a weaker correlation with the 1-OO¹H proton, indicated with a small arrow in the plot in Figure 8. The correlation with the 1-OO¹H provides unambiguous evidence for intermolecular magnetization transfer, from the hydrogenbonded proton (Figure 7). In contrast, the dipolar correlations with the nearby aromatic 3'-¹H and 5'-¹H protons are very weak, beyond the limit set by the contours in Figure 8.

Since predominantly the 4'-O¹H and the 1-OO¹H appear to contribute to the initial polarization build-up of the 4'-¹³C signal, we performed a MAS Floquet simulation for a spin system that consisted of the 4'-¹³C, the 4'-O¹H, and the 1-OO¹H (Figure 6D). The simulated LG-CP carbon spectrum was broadened by means of a Lorentzian apodization of 800 Hz, the same value that was used in the calculations of the CH and CH₂ responses in Figure 5. The higher frequency part of the experimental spectrum in Figure 6B is closely reproduced in the simulated response in Figure 6D, which corroborates our findings that mainly two protons appear to be involved in the polarization transfer to the 4'-¹³C. The shape of the higher frequency part of the LG-CP carbon spectrum is similar to the one in Figure

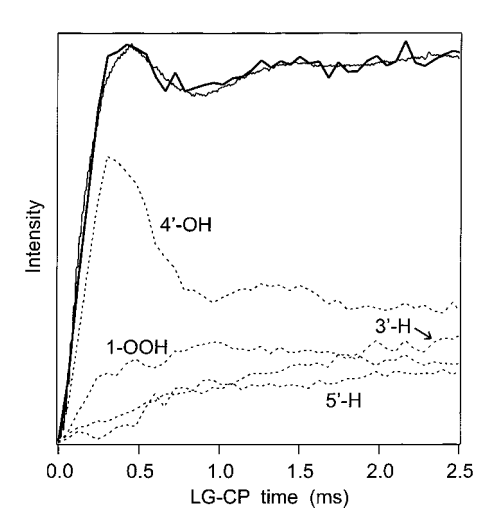


Figure 9. LG-CP build-up curves associated with the 4'-13C, extracted from a 3-D experiment recorded in a field of 14.1 T with the pulse program in Figure 2B. A MAS speed $\omega_r/2\pi = 12$ kHz was applied. The LG-CP was adjusted for the n = -1 HH condition. The slices allow for a separate study of the magnetization exchange between the 4'-13C and 4'-O1H, 1-OO1H, 5'-1H and 3'-1H. The slices are added (thick solid line) and compared with the build-up of the 4'-13C signal intensity extracted from the 2-D experiment in Figure 4 (thin solid line).

6B. On the other hand, there are also differences, like the presence of a narrow component centered around 0 Hz in the experimental response, which is absent in Figure 6D. In addition, the experimental response has wings extending to higher frequencies. This may reflect the interactions of the 4'-13C with the relatively close 3'-1H and 5'-1H, which may also take part in, for instance, relayed transfer processes of the form 3'- $^{1}H \rightarrow$ $3'-^{13}C \rightarrow 3'-^{1}H \rightarrow 4'-^{13}C$.

To disentangle the contributions from the various protons involved in each heteronuclear dipolar transfer process, a 3-D spectrum was recorded with the pulse program of Figure 2B at 600 MHz ¹H frequency, using $\omega_r/2\pi = 12$ kHz. The combination of 2-D heteronuclear (¹H-¹³C) FSLG decoupled correlation spectroscopy with variable LG-CP times in a third dimension allows for a separation of the polarization transfer events in the carbon and proton chemical shift dimensions. From the buildup of the intensities of the heteronuclear correlations with increasing LG-CP contact time, individual carbon-proton couplings can be characterized. Figure 9 shows several slices that are extracted from the 3-D experiment. The 4'-13C magnetization build-up is associated with heteronuclear dipolar interactions of 4'- 13 C with 4'- 01 H, 1- 01 H, 5'- 1 H or 3'- 1 H (Figure 9, dashed lines). The 4'-13C has the strongest interaction with the 4'-O1H proton, which gives rise to a frequency component $\Delta\omega/2\pi = 2100$ Hz. The initial polarization transfer from the 1-OO1H proton is faster than the transfer from the nearer 5'-1H and 3'-1H and is weakly oscillating with a period of about 2.0 ms, which can account for the observed weak $\Delta\omega$ $2\pi = 1150$ Hz component in Figure 6B. The thick solid line in Figure 9 is obtained by adding the separate slices and is very similar to the signal build-up of the 4'-13C extracted from the 2-D experiment (Figure 9, thin solid line). This means that the 4'-13C accepts its polarization predominantly from the 3'-1H, 4'-O1H, 5'-1H and 1-OO1H. The Fourier transforms of the polarization transfer from 5'-1H and 3'-1H to 4'-13C yield LG-CP carbon spectra that are centered around 0 Hz, hence the narrow response in the center in Figure 6B can be assigned to couplings with the 3'-1H and 5'-1H and probably involves relayed transfer of polarization.

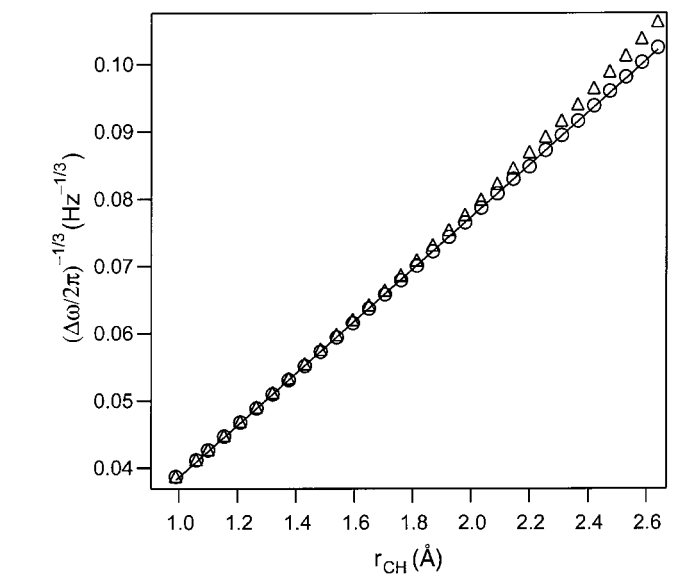


Figure 10. Simulated curves to investigate the relationship between the splitting $\Delta\omega/2\pi$ and the CH distance $r_{\rm CH}$. The simulations were performed for an isolated CH spin-pair without apodization (O) and with a 600 Hz exponential apodization (△). The solid line represents a linear computer fit.

Discussion

The LG-CP carbon spectrum of a CH moiety (Figure 5C) is symmetric around $\omega = 0$ and yields two well resolved maxima. The splitting $\Delta\omega/2\pi$ between the maxima provides a direct measure for the dipolar coupling strength and can be used to resolve internuclear ${}^{1}H^{-13}C$ distances. To translate the $\Delta\omega/2\pi$ into a heteronuclear distance r_{CH} , a set of simulations was performed for an isolated CH spin-pair, and a calibration line was produced, in a way similar to that discussed for a homonuclear spin-pair on rotational resonance by Verdegem et al.³¹ In this set, $r_{\rm CH}$ was varied in steps by shifting the proton away from the carbon along the direction of the internuclear vector connecting the spin-pair. Figure 10 shows a plot of $(\Delta\omega)$ $(2\pi)^{1/3}$ versus $r_{\rm CH}$ for the spin system. $(\Delta\omega/2\pi)^{1/3}$ varies linearly with r_{CH} (Figure 10, "O"), which can be used to extract CH distances from the data with good accuracy. The dipolar coupling strength diverges for r_{CH} approaching zero and a linear least-squares fit yields $r_{\rm CH} = a(\Delta\omega/2\pi)^{-1/3}$, with $a = 25.86 \pm$ 0.01 ÅHz^{1/3} (Figure 10, solid line). When an exponential apodization is applied to the data in the time domain (Figure 10, " Δ "), $\Delta\omega/2\pi$ decreases slightly. For instance, a 600 Hz exponential apodization yields a shift of about 50 Hz, while an apodization of 1000 Hz produces a shift of approximately 85 Hz. In these cases for large $r_{\rm CH}$ small deviations from linearity can be observed.

Correlations between quaternary carbons and protons that are not directly bonded to a carbon are remarkably easy to detect in the uniformly ¹³C enriched system. Apparently, for an ¹H directly bonded to a 13C, the magnetization is transferred coherently to its adjacent carbon in a short time of $\sim 60-100$ us (cf. Figure 5 A and B). After this initial rapid transfer period, the ¹H that are not directly bonded to a ¹³C, for instance O¹H or N¹H₃⁺, can transfer magnetization over relatively long distances. For quaternary carbons, CP will be predominantly from protons that are not strongly coupled to a ¹³C spin, like hydrogen bonded protons. This offers an attractive route for collecting heteronuclear intermolecular distance constraints in

⁽³¹⁾ Verdegem, P. J. E.; Helmle, M.; Lugtenburg, J.; de Groot, H. J. M. J. Am. Chem. Soc. 1997, 119, 169.

a multispin cluster. In favorable cases such polarization transfer can already be detected without any multipulse decoupling scheme, as was demonstrated previously for the 1-COOH and 4'-COH with the CP/WISE technique.²⁶

The two high-frequency components observed for the 4′-¹³C build-up provide information about the heteronuclear dipolar couplings of the 4'-13C with the 4'-O1H and 1-OO1H protons. The relationship between $\Delta\omega/2\pi$ and $r_{\rm CH}$ according to Figure 10 can be exploited to estimate the CH distance from the experimentally observed maxima in the LG-CP carbon spectrum. We have noted above that the effect of remote protons on the LG-CP response of a strongly coupled CH spin pair is a broadening and a slight increase of $\Delta\omega/2\pi$. Since the relationship between $\Delta\omega/2\pi$ and $r_{\rm CH}$ was obtained for an isolated spinpair, the frequency shift due to coupling to remote protons in the experiment will introduce an uncertainty in the estimated CH distances. For a strongly coupled spin-pair, this uncertainty will be small. For instance, for the CH moiety in Figure 5E, the differences in $\Delta\omega/2\pi$ for the spin-clusters containing one and five protons translate in deviations in r_{CH} that are less than 1%. On the other hand, the effect of remote protons may be larger on weakly coupled CH pairs. Artificial broadening of the simulated response will not help, since this will shift the maxima to lower frequencies, that is, in the opposite direction. Hence the best results will be obtained if we work with the straight line in Figure 10. A second uncertainty may be introduced by the scaling of the dipolar coupling in the experiment. The coupling strength $\Delta\omega/2\pi$ obtained from the experimental data is slightly lower than the $\Delta\omega/2\pi$ in the simulations. A possible origin for this discrepancy may be an experimental scaling factor that is lower than the theoretical factor $\sin(\theta_{\rm m})$. Comparing the experimental and simulated $\Delta\omega$ 2π for the 2-CH moiety in Figure 5 C and E, respectively, a correction factor of ~1.07 can be estimated for the scaling factor. The effect of this factor is small and it may result in a 2% deviation in the distance.

Taking the uncertainties in $r_{\rm CH}$ into account in the experimental error, the 2100 \pm 25 Hz frequency component yields $r_{\rm CH} = 2.02 \pm 0.04$ Å, while the 1150 \pm 100 Hz component gives a CH distance of 2.47 \pm 0.07 Å. These distances compare very well with the $r_{\rm CH} = 1.982$ Å and $r_{\rm CH} = 2.521$ Å obtained from the neutron diffraction structure (Figure 7). It demonstrates that the accuracy in the distances $r_{\rm CH}$ obtained with the

NMR is good and that the procedure can be applied to extract r_{CH} from the time-oscillating CP build-up curves. This should be particularly useful to characterize hydrogen bonded protons in a wide range of solids, including biological preparations.

Conclusions

In this work it is shown that the time-oscillatory polarization transfer during LG-CP can be analyzed to determine heteronuclear distances with good accuracy. Fourier transforms of the LG-CP build-up curves provide effective carbon spectra that resemble heteronuclear dipolar powder spectra for nonspinning samples. The LG-CP carbon spectra can be closely reproduced with MAS Floquet simulations. A set of simulations was performed with different $r_{\rm CH}$, to provide an empirical relation between the dipolar coupling strength $\Delta\omega/2\pi$ and the CH-distance. We have demonstrated that this relation can be utilized to determine $r_{\rm CH}$ from experimentally observed coupling strengths.

The pulse sequences are remarkably sturdy. An accurate measurement of distances is possible in a straightforward manner and we did not observe a pronounced sensitivity to RF mismatch or other experimental settings. The measurement of heteronuclear distances sets the stage for yet another route to *de novo* structure determination using uniformly enriched compounds or multispin clusters in ordered systems without long-range translation symmetry, for instance biological systems such as membrane proteins. In addition, a 3-D version of the technique enables an analysis of the polarization exchange within individual CH spin-pairs, offering exciting prospects to study the coherent cross-polarization dynamics and hydrogen bonding environments in detail on a microscopic scale.

Acknowledgment. We thank Professor H. Oschkinat for access to his ultrahigh field narrow bore equipment. H. Förster and C. Erkelens are acknowledged for support during various stages of the experiments. This research was financed in part by preparatory project BIO4-CT95-9048 and demonstration project BIO4-CT97-2101 of the European Commission, and Human Frontiers Science Program (HFSP) project number HFSPO-RGO 184/199. HJMdG is a recipient of a PIONIER award of the Chemical Science section (CW) of The Netherlands Foundation for Scientific Research (NWO).

JA992714J